# Exploratory analysis of voxel size effects on CT measurements of situation characteristics of type point-to-point distance

**T L Fernandes[1], G D Donatelli[1] and C R Baldo[2]**

[1] Centre for Metrology and Instrumentation - CMI, Reference Centres for Innovative Technologies - CERTI, Florianópolis, SC, Brazil
[2] Centre for Engineering, Modelling and Applied Social Sciences - CECS, UFABC - Federal University of ABC, Santo André, SP, Brazil

E-mail: thf@certi.org.br

**Abstract**. In recent years, computed tomography (CT) has been applied as an industrial metrology tool for the dimensional evaluation of visible and even hidden features of production parts in a non-destructive manner. Considering the experimental findings of a recent work of the authors, this paper deals with the effect of voxel size on measuring distances between feature-of-size centers, which would be less sensitive to edge offset errors. Particular attention is given to the design of experiment and to the measurement uncertainty sources. The most significant experimental findings are outlined and discussed in this paper.

## 1. Introduction

In recent years, computed tomography (CT) has been applied as an industrial metrology tool for the dimensional evaluation of visible and even hidden features of production parts in a non-destructive manner. CT features great operational advantages over existing coordinate metrology techniques, as tactile and optical coordinate measuring machines.

However, CT working principle and scanner setup give rise to many influence factors that affect the performance of dimensional evaluations. They are related to the X-ray source (e.g. photon energy, focal spot size), the detector (e.g. response time, pixel size, exposure time, image averaging), the CT kinematics (e.g. magnification and rotation axis repeatability and accuracy), the object (e.g. size, shape, material), and the mathematical data processing (e.g. artefact correction, segmentation, measuring strategy, fitting algorithm) [1].

When choosing a CT scanner for composing the dimensional metrology infrastructure of an organization, VDI/VDE 2630 Part 1.3 can be very useful, since it defines specifications and methods for acceptance testing of coordinate measuring machines with sensors relying on the X-ray CT principle. The dimensional performance of the CT system is investigated by measuring the distance between two balls centers. Although this approach is considerably robust for comparison purposes, as it is nearly insensitive to threshold errors, it is not useful for measurement uncertainty estimation of CT-based data [2].

A recent technical paper of the authors brought some lessons learnt for more reliable dimensional analysis of feature of size, through an exploratory study using modular test artefacts [3]. Two of the lessons learnt are replicated here: (a) the focal spot size should be closer or smaller than the voxel size; (b) the higher the magnification factor, the lower the measured biases.

The first experimental lesson learnt agrees with the definition of geometric unsharpness (blurring), from which the focal spot size must be correlated with the voxel size prior to measurement [4]. The second lesson learnt is the subject matter of this paper, but focusing on distances between feature-of-size centers, which would be less sensitive to edge offset errors.

## 2. Case description

### *2.1. Test object situation characteristics*

The test object selected for this exploratory study is made of acetal photopolymer (POM) and composed of a pattern of holes uniformly spaced. The distances between each circle center related to the reference circle center define the situation characteristics to be evaluated. This feature arrangement is suitable for investigating the voxel size effect on center-to-center distance measurement. This arrangement is also adequate for assessing the length-dependent error behavior, since it covers different distances.

Figure 1 shows the test object and the situation characteristics. All center-to-center distances are related to situation feature (hole center) 1, namely: $L_{12}$ (distance between situation features 1 and 2). The same reasoning applies to the other situation characteristics: $L_{13}$, $L_{14}$, $L_{15}$ and $L_{16}$.

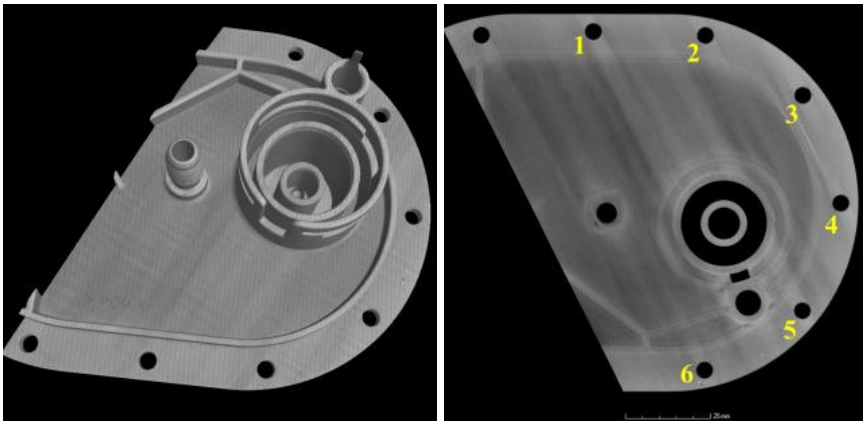


**Figure 1.** Illustrative image of the test object and the situation characteristics (distances between a given circle center and the reference circle center no. 1).

## 3. Measurement setup

### *3.1. Tactile reference measurements*

The situation characteristics of the test object were calibrated on a Carl Zeiss PRISMO ultra CMM, which is housed in a temperature-controlled room kept at (20.0 ± 0.3) °C. All situation characteristics were realized by associating ideal features of type circle to the sampled points (using least-squares method), from which the situation characteristics (point-point distance) were derived. Measurement uncertainties were estimated by using the Virtual CMM software output as well as expert judgment. Table 1 lists the calibration results.

### *3.2. CT measurements*

The test objected was measured on a Carl Zeiss METROTOM 1500 CT system, which is equipped with a 225 kV micro-focus tube and a $2048^2$ pixels flat panel detector. The CT system is installed in a temperature-controlled room kept at (20 ± 1) °C. The CT system manufacturer specifies a MPE for length measurements of (9 + L/50) µm, using a test piece consisting of 27 ruby spheres mounted on carbon fiber shafts, and calculating the center-to-center distances of several pairs of spheres from the CT data [2]. This approach is on the other hand nearly insensitive to material influence [3].

**Table 1.** Calibration results for the object intrinsic characteristics (best estimates and expanded uncertainties in millimeters).

| Feature | Calibration results |
|---|---|
| $L_{12}$ | 33.070 ± 0.002 (k = 2) |
| $L_{13}$ | 64.610 ± 0.002 (k = 2) |
| $L_{14}$ | 88.867 ± 0.002 (k = 2) |
| $L_{15}$ | 102.941 ± 0.002 (k = 2) |
| $L_{16}$ | 105.243 ± 0.002 (k = 2) |

Due to the high aspect ratio (width-to-thickness ratio) of the test object, special attention to find the proper object orientation had to be taken, in order to avoid saturation or dying out of pixels during capture of the X-ray images. To scan the object, the source voltage was set high enough to avoid beam extinction, and detector integration time set to a convenient value. The source current was then tuned to enhance image contrast / brightness. The number of angular poses was chosen as about the number of pixels covered by the resulting shadow of the test object in the projection.

The magnification axis was, in the first attempt, positioned to project the part using the maximum possible area of the detector (and thus reducing the voxel size). For the second experimental trial, the magnification factor was halved (thus enlarging the voxel size by a factor of two). Table 2 shows the CT settings for each experimental trial.

**Table 2.** Simplified list of the CT control settings chosen for scanning the test object under analysis.

| Parameter | Unit | Trial 1 | Trial 2 |
|---|---|---|---|
| Source voltage | kV | 120 | 120 |
| Source current | µA | 450 | 450 |
| Focal spot size | µm | 54 | 54 |
| Integration time | s | 1 | 1 |
| Detector binning | -- | 2x2 | 2x2 |
| Magnification | -- | 2.50 | 1.25 |
| Voxel size | µm | 160 | 320 |
| No. of projections | -- | 800 | 800 |

Regarding the surface definition from the voxel dataset, the standard ‘iso-50%’ threshold value was applied globally. From the material boundary thus defined, 3600 points evenly spaced around the circumferential line were extracted for each situation feature, and the ideal feature of the type circle associated to the extracted points using the least-squares fitting method.

## 4. Experimental results

Measurements performed on the CT system were repeated three times for each experimental trial. For each characteristic under analysis, the mean value of the measurement result and the standard uncertainty associated with measuring procedure were computed. The object temperature inside the CT system enclosure was monitored in order to properly compensate temperature effects and to assess the standard uncertainty associated with the systematic error. For more information regarding the experimental uncertainty evaluation, please refer to ISO 15530-3.

Table 3 shows the resulting individual standard uncertainties, expanded uncertainty and bias (after temperature correction) for each characteristic of the test object. Since the dominant factors were the calibration uncertainty and procedural uncertainty, which were nearly identical for all characteristics, the expanded uncertainty after correcting the bias would be virtually the same, $U = 0.005$ mm.

The metric normalized error (En-value) was calculated using the expanded uncertainty and bias absolute difference (table 3), which confirmed that the situation characteristic measuring difference related to each trial are not statistically identical, as the En-values are beyond the range [0,1]. That significant bias difference is a direct effect of the voxel size chosen for each experimental setup.

**Table 3.** Uncertainty components, bias difference and normalized error related to each situation characteristic (values in millimeters).

| | Situation characteristic | | | | |
|---|---|---|---|---|---|
| Component | $L_{12}$ | $L_{13}$ | $L_{14}$ | $L_{15}$ | $L_{16}$ |
| $u_{cal}$ | 0.001 | 0.001 | 0.001 | 0.001 | 0.001 |
| $u_p$ | 0.002 | 0.002 | 0.002 | 0.002 | 0.002 |
| $u_b^{(1)}$ | 0.000 | 0.001 | 0.001 | 0.001 | 0.001 |
| $U\,(k = 2)$ | 0.005 | 0.005 | 0.005 | 0.005 | 0.005 |
| $\lvert b_1 - b_2 \rvert$ | 0.018 | 0.024 | 0.029 | 0.024 | 0.024 |
| En | 2.86 | 3.64 | 4.25 | 3.42 | 4.76 |

$u_{cal}$ standard uncertainty of the parameter of the calibrated workpiece
$u_p$ standard uncertainty of the measurement procedure
$u_b$ standard uncertainty of the systematic error (bias)
$u_b = D_i \,.\, (T - 20\ °C) \,.\, u_\alpha :: \alpha = 92 \,.\, 10^{-6}\ °C^{-1} \pm 15\%$ and $T = (21.4 \pm 0.2)\ °C$
b systematic error observed during uncertainty evaluation

Figure 2 graphically shows the bias divergence between experimental trials 1 and 2. By not using the maximum possible area of the detector in trial 2, and therefore lowering the structural resolution, measurement results were adversely affected. In fact, the observed measurement bias exceeded the MPE for length measurements specified by the CT system manufacturer.

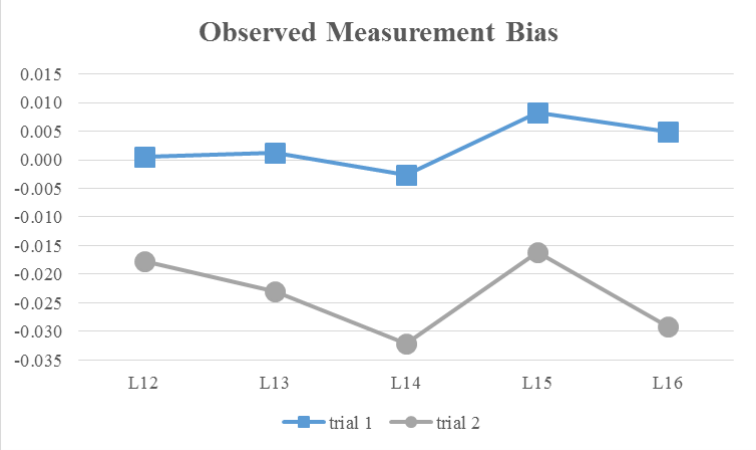


**Figure 2.** Chart of the observed bias for each experimental trial (point-to-point distance).

Although poorer structural resolution was a direct consequence of arbitrarily positioning the test object closer to the detector, in practice this effect can be very common, e.g., when scanning a test object that resembles a stepped cylinder [5].

## 5. Concluding remarks

In this paper, the effect of changing the voxel size (by changing the image magnification factor) was analyzed for some situation characteristics. By worsening the structural resolution, measurement accuracy was seriously undermined. This may be attributed to insufficient sampling at the image level (so-called aliasing artefacts) [1].

The proper location and orientation of the test object is an important duty of the CT metrologist. Finding the optimal CT setup may not be a trivial task, as the measurement error behavior depends on the workpiece material and geometry. The use of reference workpieces, either calibrated using a CMM or a CT system with multiple measuring sensors, makes possible improving CT measuring accuracy by correcting known systematic effects.

## References

[1] Kruth J P, Bartscher M, Carmignato S, Schmitt R, Weckenmann A and De Chiffre L 2011 Computed tomography for dimensional metrology *CIRP Annals* **60(2)** 821-42

[2] Hiller J, Maisl M and Reindl L M 2012 Physical characterization and performance evaluation of an x-ray micro-computed tomography system for dimensional metrology applications *Meas. Sci. Technol.* **23** 085404

[3] Baldo C R, Fernandes T L and Donatelli G D 2015 Experimental investigation of computed tomography dimensional capability using modular test parts *XXI IMEKO World Congress* Prague CZ

[4] Weiss D, Shi Q and Kuhn C 2012 Measuring the 3D resolution of a micro-focus X-ray CT setup *CTC* Wels AT

[5] Krämer P and Weckenmann A 2010 A Multi-energy image stack fusion in computed tomography *Meas. Sci. Technol.* **21** 045105